


Capturing B Type Acute Lymphoblastic Leukemia Cells Using Two Types of Antibodies

Kutay İçöz 

BioMINDS (Bio Micro/Nano Devices and Sensors) Lab, Dept. of Electrical and Electronics Engineering, Abdullah Gül University, Kayseri, Turkey
Bioengineering Dept., Abdullah Gül University, Kayseri, Turkey

Tayyibe Gerçek

BioMINDS (Bio Micro/Nano Devices and Sensors) Lab, Dept. of Electrical and Electronics Engineering, Abdullah Gül University, Kayseri, Turkey
Bioengineering Dept., Abdullah Gül University, Kayseri, Turkey

Ayşegül Murat

Genome and Stem Cell Center (GENKOK), Erciyes University, Kayseri, Turkey

Servet Özcan

Biology Dept., Erciyes University, Kayseri, Turkey
Genome and Stem Cell Center (GENKOK), Erciyes University, Kayseri, Turkey

Ekrem Ünal

Pediatric Oncology Dept., Erciyes University, Kayseri, Turkey

DOI 10.1002/btpr.2737

Published online November 20, 2018 in Wiley Online Library (wileyonlinelibrary.com)

One way to monitor minimal residual disease (MRD) is to screen cells for multiple surface markers using flow cytometry. In order to develop an alternative microfluidic based method, isolation of B type acute lymphoblastic cells using two types of antibodies should be investigated. The immunomagnetic beads coated with various antibodies are used to capture the B type acute lymphoblastic cells. Single beads, two types of beads and surface immobilized antibody were used to measure the capture efficiency. Both micro and nanosize immunomagnetic beads can be used to capture B type acute lymphoblastic cells with a minimum efficiency of 94% and maximum efficiency of 98%. Development of a microfluidic based biochip incorporating immunomagnetic beads and surface immobilized antibodies for monitoring MRD can be an alternative to current cost and time inefficient laboratory methods. © 2018 American Institute of Chemical Engineers Biotechnol. Prog., 35: e2737, 2019

Keywords: B type acute lymphoblastic leukemia cells, cell capture efficiency, minimal residual disease, immunomagnetic separation, two antibody sorting

Introduction

Currently there is no absolute way to prevent leukemia; but there are different treatments for patients such as drug therapy (chemotherapy), bone marrow transplantation, radiation treatment, and immunotherapy.¹ Among these methods, chemotherapy is the widely used first line treatment but results differ from patient to patient. Some of the treated patients with chemotherapy achieve remission; however, the cancer cells of some patients are resistant to treatment. The resistant cancer cells (blast cells) can cause relapses and repeat the cancer known as minimal residual disease (MRD).² Current treatment protocols monitor the MRD of the patients with acute lymphoblastic leukemia (ALL) during and after the chemotherapy treatment, which is an important indicator for survival rate for the patient. According to these protocols in the case of positive

MRD detection, intensive chemotherapy is applied. Today flow cytometry (FC) and polymerase chain reaction (PCR) are the two laboratory techniques used for MRD detection.³ The antigens CD19, CD34, and CD10 are the main biomarkers for detecting MRD using FC.⁴ Together with these three antigens, the combination of CD38, CD45, CD22, and CD58 antibodies could be also added to panel to detect MRD cells.^{4,5} However, FC and PCR are expensive methods and require experienced personnel. The drawbacks of FC and PCR stimulate the development of alternative approaches such as microfluidic platforms.^{6,7} Microfluidic based chips have been developed to *in vitro* detect rare tumor cells using various microfluidic designs.^{8–10} Some of the microfluidic systems incorporate immunomagnetic particles (magnetic micro/nanoparticles coated with antibodies) to capture cancer cells.^{11–13} Immunomagnetic particles have prominent advantages because of the fact that they do not only provide separation of target molecules but also can be incorporated with mechanical,^{14,15} optical,^{16,17} and electrochemical^{18,19} methods to enhance sensitivity.

Correspondence concerning this article should be addressed to K. İçöz at kutay.icoz@agu.edu.tr

Our future goal is to develop a method that integrates immunomagnetic beads and microfluidic channels to monitor MRD (MRD Biochip). For the leukemic cells, the detection limit of cytomorphology is 10^{-1} – 10^{-2} and FC and PCR based methods is 10^{-4} – 10^{-5} .²⁰ The target of MRD Biochip is to reach a detection limit of 10^{-3} by capturing the leukemic cells having three main surface biomarkers. The first version of the MRD Biochip will not be as sensitive as FC but it can be a low-cost and easy to use alternative to FC in low-income countries where MRD monitoring is not routinely performed.

In order to construct the MRD Biochip, firstly the binding efficiency of immunomagnetic beads to B type acute lymphoblastic leukemia (B-ALL) cells and secondly forming sandwich assays by capturing cells on functionalized surfaces have to be investigated. For this purpose we tested two types of magnetic beads, 120 nm size and 4.5 μ m size, coated with different antibodies specific to the CD19, CD34, CD10, and CD45 membrane antigens. Screening cells for one surface marker is not sufficient for MRD monitoring. Our strategy was to use two cell surface markers; either double immunomagnetic sorting or single immunomagnetic sorting combined with capturing the cells on antibody functionalized gold surface. Screening two surface markers of tumor initiating cells by using immunomagnetic beads and nonmagnetic beads was previously demonstrated where CD24 nonmagnetic beads were used to bind to CD24⁺ cells and saturate the cell surface to block the binding of CD44 magnetic beads. Thus, only immunomagnetic separation of CD44⁺/CD24⁻ cells was established.²¹

After the immunomagnetic separation step, in order to investigate the binding of the cells on a functionalized gold surface and to calculate the capture efficiency we used quartz crystal microbalance (QCM). QCM sensor is an ultrasensitive technique that has been also used to investigate tumor cell properties such as adhesion²² and drug resistance.²³

Our experiments are depicted in Figure 1 and composed of three sets. In the first set, binding efficiencies of various immunomagnetic beads to B lymphoblast cells were investigated. In the second set, double sorting was performed where two different immunomagnetic beads were applied to bind

cells. In the third set, real-time QCM measurements were performed. For QCM measurements in order not to cause any clogging in the tubes, nanosize immunomagnetic beads were used for separation and captured cells were introduced to the sensor surface which was functionalized with CD19 antibody. One of the aims of the QCM experiments is to simulate the surface capture experiments for the MRD Biochip. The MRD Biochip will have gold surfaces fabricated in the microfluidics channels and these gold surfaces will be functionalized with the antibodies to capture leukemic cells as tested in QCM experiments.

The initial cell amount and the cells (noncaptured) in the washing solutions were counted using the Muse cell counter and manual cell counting. By using the difference of the initial cell amount and the noncaptured cell amount, the capture efficiency was determined (Eq. 1).

$$\text{Capture Efficiency} = \frac{\text{initial cells} - \text{noncaptured cells}}{\text{initial cells}} \times 100 \quad (1)$$

In the next sections, we explain the materials, methods and the experimental results and finally conclude with the discussion.

Materials and Methods

Immunomagnetic beads of 120 nm in diameter coupled with monoclonal antihuman antibody were purchased from Miltenyi Biotec (Auburn, CA). Immunomagnetic beads of 4.5 μ m in diameter coupled with monoclonal antihuman antibody (Dynabeads) were purchased from Thermo-Fisher (Waltham, MA). B lymphoblast cells CCRF-SB cell line was purchased from American Type Culture Collection (Rockville, MD). After receiving the cell line from ATCC, cells were thawed, washed and grown exponentially with supplementation of 10% serum as suggested by the vendor at 37 °C and 5% CO₂ atmosphere under sterile conditions. Is cove's Modified Dulbecco's Medium or Roswell Park Memorial Institute-1640 medium, serum, and trypsin were purchased from Biological industries

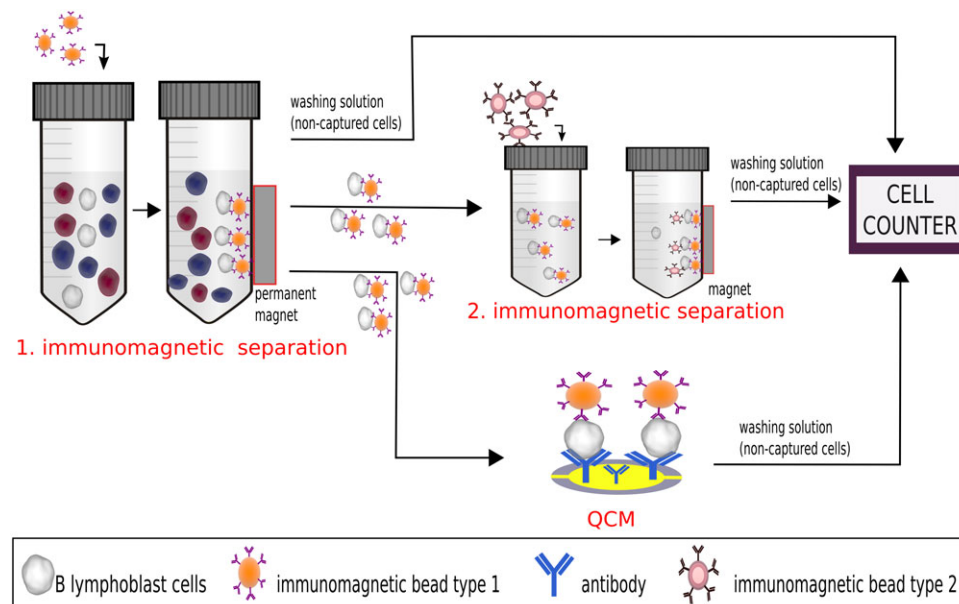


Figure 1. Illustration of the experiments; immunomagnetic separation, QCM measurements, and double sorting.

(BI, Israel). Penicillin, L-glutamine, and the other chemicals were acquired from Sigma–Aldrich (St. Louis, MO).

The immunomagnetic bead manufactures suggests incubation time and bead amounts for efficiently capturing cells; however, we performed our own optimization experiments, tested manufacturer suggestions and determined the parameters.

Nanosize immunomagnetic bead separation

In order to prepare the buffer solution, 0.5% bovine serum albumin (BSA) was added into 10 mL of AutoMACS buffer, which includes Dulbecco's Phosphate Buffered Saline (DPBS) in pH 7.2 value and 2 mM ethylenediaminetetraacetic acid (EDTA). A gentle pipetting disassociated cell clusters and then 5 mL of cell culture was taken from the flask into a 15 mL falcon tube and was centrifuged for 5 min. After aspirating the supernatant, 5 mL of DPBS was added for washing the cells. Initial number of cells was determined before immunomagnetic separation. After counting the cells, 5×10^5 cells/mL was taken from the cell-DPBS solution and was centrifuged for 10 min at room temperature. Supernatant was aspirated and pellet was resuspended with 80 μ L of buffer. Twenty microliters of CD19 Microbeads (Miltenyi) or CD45 Microbeads (Miltenyi) was added and mixed by rotating in 4 °C for 15 min as manufactured suggested. After 15 min of incubation, cells were washed by adding 2 mL of buffer and centrifuged for 10 min at 300g. Supernatant was aspirated and pellet was resuspended with 500 μ L of buffer. MiniMACS (Miltenyi) separator was placed onto the MACS (Miltenyi) stand. MiniMACS column was placed in the separator. The column was prepared by rinsing with 500 μ L of buffer. The cell suspension was applied into the column. Unlabeled cells that eluted were collected as a negative fraction in a six well plate. Column was washed four times with 500 μ L of buffer. The column was removed from the magnetic field and placed on a suitable collection tube and 1 mL of buffer was pipetted onto the column. Pushing the plunger into the column flushed out magnetically labeled cells.

Microsize immunomagnetic bead separation

The buffer was prepared by adding 0.1% BSA and 2 mM EDTA to DPBS without calcium and magnesium in pH 7.4. All beads were stored in 4 °C. Dynabeads were first mixed by a rotator at room temperature for 5 min inside of a falcon tube (50 mL) in order to homogenize the beads. One milliliter of the buffer was added to a 2 mL of Eppendorf tube. Twenty-five microliters of CD19 Dynabeads or 40 μ L of CD45 Dynabeads was added into the tube and mixed gently. This bead solution was placed into a magnetic separation rack and washed with buffer three times. After counting, 5×10^5 cells/mL was taken from the cell-DPBS solution and was centrifuged for 10 min. Supernatant was aspirated and pellet was resuspended with 1 mL of buffer. These cells were added into a prewashed 25 μ L of CD19 Dynabeads or 40 μ L of CD45 Dynabeads and mixed by rotating in 4 °C (as manufacturer suggested) in 20 min. After 20 min of incubation, cells were ready to separate into unlabeled and labeled ones. This cell suspension was placed into the magnetic separator. After 2 min of waiting, 1 mL of buffer solution was aspirated and unlabeled cells were collected into a six well plate. The tube was removed from the separator and 1 mL of buffer was added and mixed gently. The washing steps were repeated three times and 1 mL of buffer was added.

Cell counting

Cell counting was performed by using Muse Cell Analyzer (Millipore, Billerica, MA) and manually by using a Neubauer Chamber (Sigma–Aldrich). For each experiment initial number of cells, the numbers of cells (noncaptured cells) in the washing solution of immunomagnetic separation (single or double sorting) or in the washing solution of surface capture experiments were counted using the both methods. The capture efficiency was calculated using the initial number of cells and the noncaptured cells in the washing solutions. Most of the cells are captured either by the immunomagnetic beads or by the antibodies immobilized on the surface.

QCM measurements

A QCM with dissipation monitoring QCM-D (Q-Sense E4, Biolin Scientific, Västra Frölunda, Sweden) together with gold-coated quartz crystals, that is, sensor chips (a fundamental frequency of 5-MHz) were purchased from Biolin and used according to the manufacturer's instructions. New sensor chips were cleaned before every experiment. Each sensor was first rinsed with deionized water and absolute ethanol then dried under a nitrogen stream. The chips were next placed in an UV/ozone chamber for 20 min, and incubated in base piranha solution (20 mL ammonia solution, 20 mL hydrogen peroxide in 30 mL deionized water) for 20 min then rinsed with deionized water, and dried under a nitrogen stream and the cleaned chip was mounted into the QCM-D chamber. The flow rate was set to 100 μ L/min and tubing with inner diameter of 0.38 mm was used to pump the cells into the chamber. The closed loop pumping performed until the surface was saturated (no frequency was change observed).

Statistics

Each experiment was repeated at least five times to obtain the means and standard deviations of the data; the error bars indicate the standard deviation from the average values. Independent samples *t*-test was performed for the experimental results. Statistical significance was considered at $P < 0.05$.

Results

Separation efficiency of single sorting

Immunomagnetic beads coated with CD10, CD19, CD45, CD34, and CD38 were tested to capture B lymphoblast cells. The CD10 and CD34 beads resulted in low yield. In order to investigate this low yield, the surface antigens of B lymphoblast cells were examined using FC. The FC measurements revealed that CD10 and CD34 antigen presence on the cells were lower than 10% and thus immunomagnetic beads coated with CD10 or CD34 could not bind to the cells. It was reported that expression of cell surface antigens for leukemia cells may differentiate when the cells are in peripheral blood or in bone marrow²⁴ or *in vitro*.²⁵ Because FC measurements verified that CD10 and CD34 antigens did not present on the cells, the immunomagnetic beads (nano and microsize) coated with CD19 and CD45 were studied (Figure 2). CD45 coated nanosize beads have higher capture efficiency approximately 98.5% and this efficiency statically differs from the capture efficiencies of other type of immunomagnetic beads.

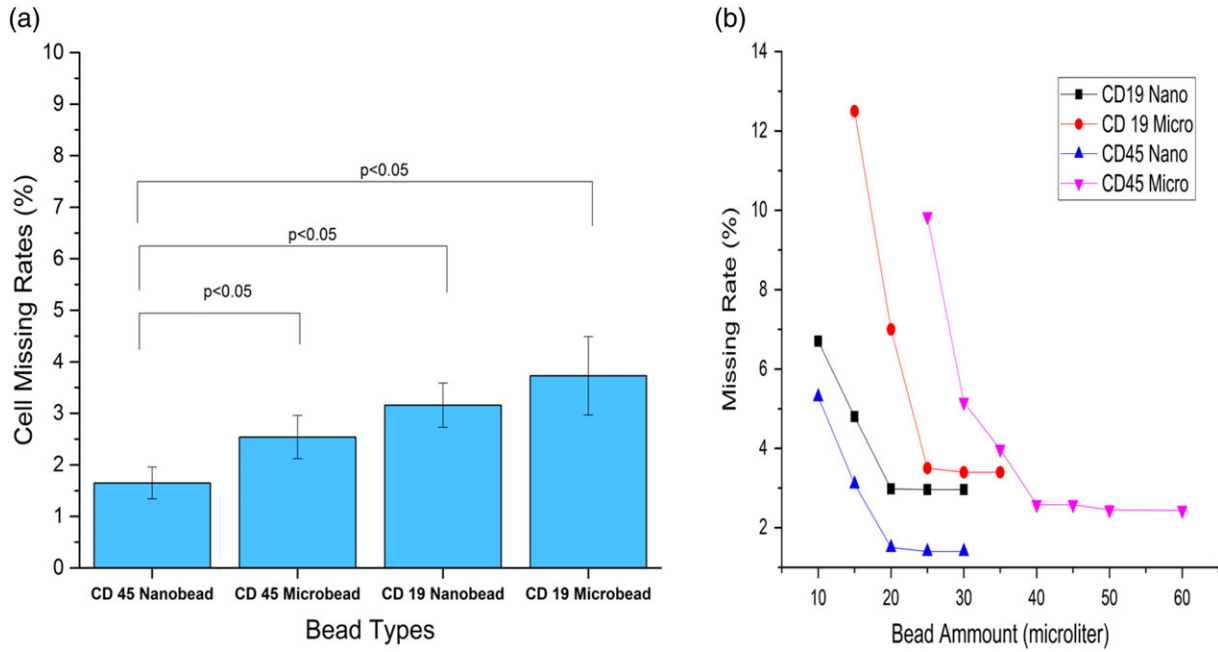


Figure 2. (a) Single sort results: CD45 or CD19, nanobead or microbead missing percentages. Between CD 45 nanobead and other experiments ($P < 0.05$), for other combinations ($P > 0.05$). (b) Bead amount optimization results.

Also microsize CD38 antibody coated immunomagnetic beads were tested and the cell-missing rate was determined as 7.7% and was not included in Figure 2.

Separation efficiency of double sorting

After the first immunomagnetic separation to test the binding of secondary antibody, second immunomagnetic separation was performed. For this purpose nanosize beads (CD45 or CD19)

were chosen for the first immunomagnetic separation and for the second immunomagnetic separation micro or nanosize bead combinations (CD45 or CD19) were tested (Figure 3).

The experimental results reveal that the combination of CD19 nanobead and CD45 microbead has the highest missing rate when compared to the other combinations. Because the cell missing rate for CD45 immunomagnetic beads was lower than CD19 immunomagnetic beads starting with the CD45 beads and then applying CD19 beads resulted in the lowest missing rate approximately 1.5%–2%.

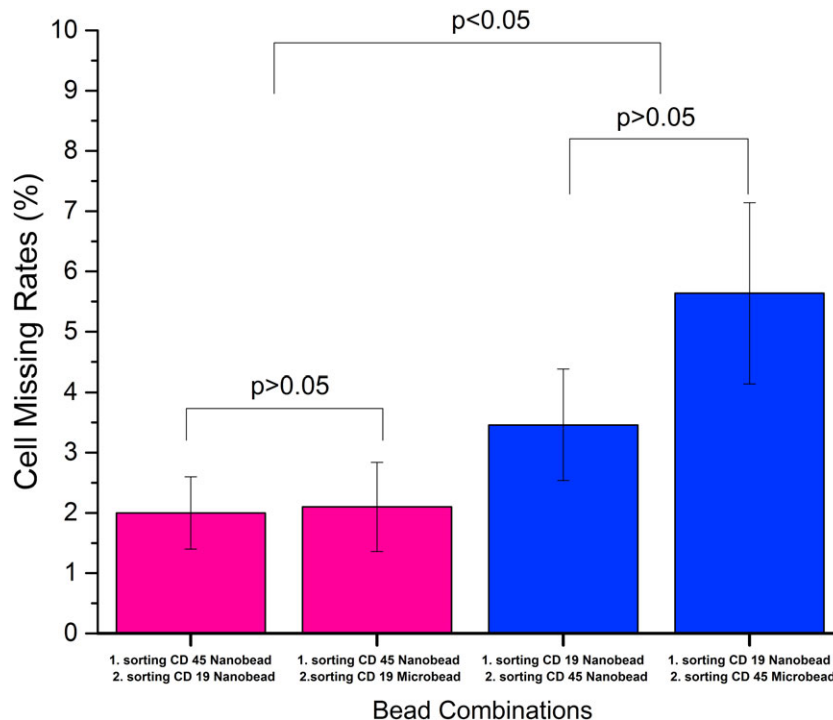


Figure 3. Double sort results: CD45 and CD19 nano and microbead missing percentages. Within the CD45 nanobead combinations and CD19 nanobead combinations ($P > 0.05$). Between the CD45 and CD19 nanobead combinations ($P < 0.05$).

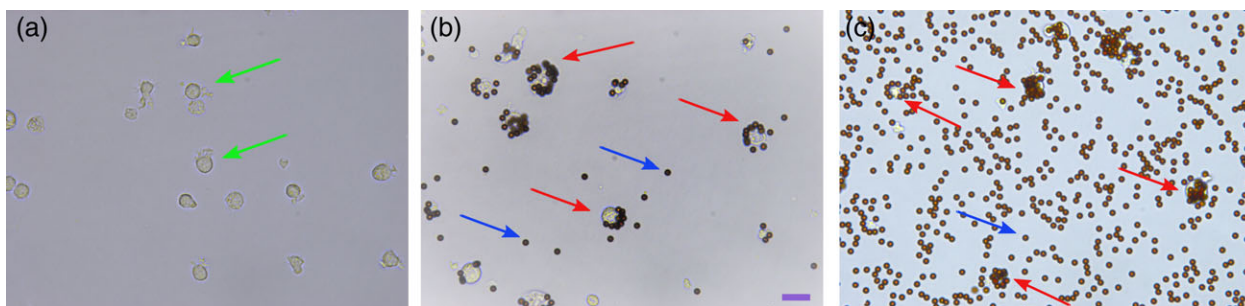


Figure 4. Bright-field optical micrographs of the separated cells. (a) After CD19 nanobead separation. Green arrows indicate the cells. (b) After CD45 microbead separation. Blue arrows indicate the single micron beads. Red arrows indicate the captured cells with microbeads. (c) After CD45 nanobead and CD19 micro bead separation. Blue arrows indicate the single micron beads. Red arrows indicate the captured cells with microbeads. Arrows are not placed for all entities. Scale bar is 20 μm and valid for all images.

To visualize the cells and immunomagnetic beads the captured cells were imaged using an optical microscope (Figure 4). Contrast to the nanobeads which are not visible under optical microscope, micro beads have uniform shape and size.

Single sorting and surface capturing

The third sets of experiments were performed to test capturing B lymphoblast cells on a solid surface. The QCM sensor surface was functionalized as reported in our previous work.²⁶ After the first immunomagnetic separation of B lymphoblast cell with CD45 nanobeads, the captured cells were introduced to the QCM chamber where CD19 antibody was immobilized on the surface. The layers on the gold surface are 11-mercaptopundecanoic acid \gg N-Ethyl-N'-(3-dimethylaminopropyl) carbodiimide hydrochloride/N-hydroxysulfosuccinimide \gg protein G \gg CD19 and the B lymphoblast cells bound to immunomagnetic beads coated with CD45 antibody. The frequency shifts of the QCM clearly show the binding events (Figure 5).

The protein G layer resulted in an average of 6.83 Hz frequency shift and oriented the CD19 antibody for higher binding efficiency. CD19 antibody caused an average of 9.3 Hz frequency shift and then the sensor surface was incubated with BSA to prevent the unspecific binding of cells. The captured cells resulted in 39 Hz frequency shift (Figure 5). The purpose of the QCM measurements was to validate the double antibody binding to B lymphoblast cells. CD19 was immobilized on the gold surface and captured the cells already bound to the CD45 nanobeads. The initial number of cells and the cells in the washing solution from the QCM chamber were counted. Cell missing rate was determined as 2.43%.

Discussion and Conclusion

The immunomagnetic separation of ALL has been demonstrated using surface antigens such as CD10,²⁷ CD19 antigen²⁸ or cocktail of CD19 and CD10.²⁹ In,²⁸ the efficiency of CD19 immunomagnetic bead separation efficiency was reported as 91%–98% which is in good agreement with the experimental results reported in this study. Even though CD10 and CD34 have prognostic value for ALL,³⁰ the B lymphoblast cells in our cell culture slightly had these antigens. This situation could be extrapolated that *in vitro* conditions could change the antigen expression of the cells.³¹ FC measurements

showed that cells are positive for CD19 and CD45 and thus we focused on these antibodies. The highest cell capture efficiency was obtained when CD45 antibody was used. In our case, in order to investigate the presence of two-antigens on the cells, first CD45 antibody and then CD19 antibody should be tested. For CD45 antibody, the nanosize beads captured higher cells compared to microsize beads. It was reported that in³² for *Escherichia coli* separation nanosize beads have higher capture efficiency compared to microsize beads. In³³ for *Salmonella* separation it was reported that micro and nanosize beads have similar analytical performance and nanosize beads have slightly better limit of detection. In the literature,^{34,35} it was stated that magnetic nanosize beads have a higher efficiency for separation when compared to microsize

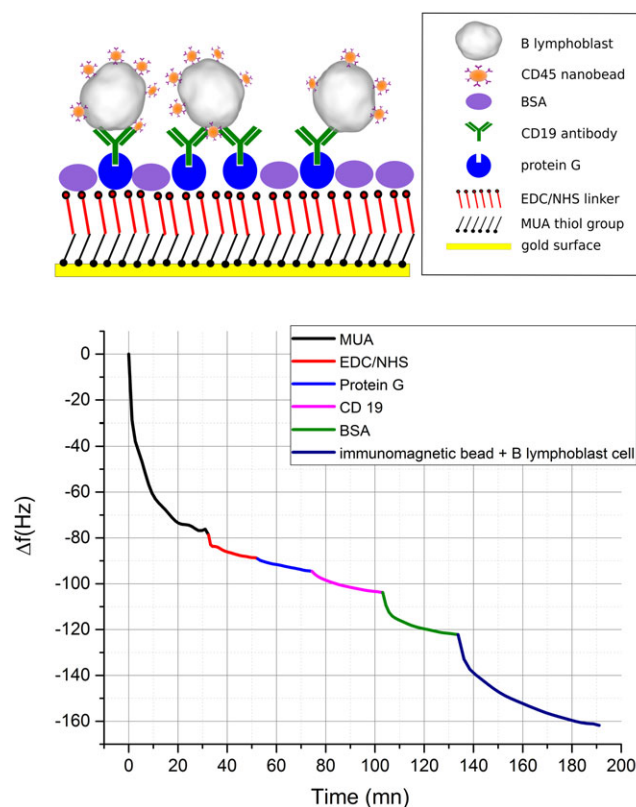


Figure 5. The QCM frequency shifts of the main steps for the CD19 immobilization and capturing the B lymphoblast cells after the first immunomagnetic separation.

beads; however, long-term stability and uniformity are some of the disadvantages of nanosize beads.

In our experiments nanosize CD45 beads showed the lowest missing rate, microsize CD45, nanosize CD19, and microsize CD19 were not statistically different. We also tested microsize CD38 antibody coated beads, however, missing rate was more than 7%. The reported missing rates were the results of optimized parameters; incubation time and immunomagnetic bead amount. Although manufactures have recommendations for these parameters, experimental validations were necessary. Because CD45 nanosize beads had the best cell capture performance, CD19 antibody was immobilized on the QCM sensor surface and double sorting performed on the QCM sensor surface. Binding to the target cells through secondary antibody either on a solid surface or on immunomagnetic beads have approximately 2% missing rate. These results show the potential of a microfluidics based biochip for monitoring MRD. Our next efforts will be to develop the biochip for MRD monitoring as a low-cost and time efficient method.

As mentioned in the previous sections, we first performed optimization experiments to determine the bead amounts and the incubation time (Figure 2). As seen in Figure 4B,C there are excessive immunomagnetic beads, which did not bind to any cells. In order not to miss any cells because of lack of immunomagnetic beads, we did not lower the bead amount and kept it at the saturation level. The results of these experiments guided us to perform experiments on the patient samples (ongoing work). The cells in the patient samples were first counted and the added bead amounts were determined using the optimization results explained in this manuscript. In the literature, immunomagnetic beads coated with CD19 or CD45 were used to separate target cells from whole blood for clinical studies.^{36–39} These findings suggest that immunomagnetic separation can be efficiently applied to patient samples. For future, real time use of this methodology will be applied to the use of whole blood samples. For doing this, we will first separate the peripheral blood mononuclear cells by using density gradient centrifugation. The obtained buffy-coat are going to be the subject of this work. In literature, there are number of studies that describes the efficient use of this technology for most cells of the immune system in humans and mice, monoclonal antibodies are available that can be used for positive or negative sorting strategies.^{40–43} According to information which are mentioned above, we do not predict any undesirable or irrelevant interaction of antibody that was specifically raised against to certain type cell, while working on homogeneous or mixed populations of cells like whole blood.

One advantage of microsize beads is to clear visibility under the bright field microscope; hence, an automated image-processing algorithm can be used to detect them. However, nanosize beads have higher capture efficiency and another advantage of nanosize beads is they do not saturate the cell surface and hence allow other type of immunomagnetic beads to bind the same cell surface.⁴¹ In the future, we are planning to test binding to more surface markers using nanosize beads coated with different antibodies. There are strategies developed for multiple immunomagnetic sorting such as positive/negative selection and enzymatic release of magnetic beads after the first separation⁴¹ which can be also applied to our experiments.

Manufacturers of micro and nanosize beads suggest, their own magnetic stands for the separation step. Magnetic racks are used for separating microsize beads and magnetic columns are used for separating nanosize beads. We tested magnetic

racks for nanosize beads and observed that the magnetic field generated by the magnetic rack was not sufficient to separate nanosize beads and conjugated cells (the separation efficiency was 0%). This magnetic selectivity is actually a benefit for double sorting to separate the cells, which are only CD45+ and CD19+. However, for the case of multiple sorting using only nanosize beads, same separation columns were employed and CD45+ or CD19+ cells were separated. These findings suggest that in the microfluidic platform one type of antibody can be immobilized to the gold surface, and target cells can be double sorted using first nanosize beads and then microsize beads coated with different antibodies. Fluid flow in the channel and the magnetic selectivity because of the magnetic stands will result in capturing cells only having three different surface markers.

Acknowledgments

Authors acknowledge The Scientific and Technological Research Council of Turkey (TÜBİTAK Project No: 115E020) for financial support and Prof. Ahmet Eken and Prof. Musa Karakucukcu from Erciyes University for valuable discussions for the cell line and immunomagnetic separation related issues. Ekrem Unal acknowledges Gilead Research Scholarship program.

Literature Cited

- Pui C-H, Evans WE. Treatment of acute lymphoblastic leukemia. *N Engl J Med.* 2006;354:166–178.
- Hauwel M, Matthes T. Minimal residual disease monitoring: the new standard for treatment evaluation of haematological malignancies? *Swiss Med Wkly.* 2014;144.
- Basso G, Veltroni M, Valsecchi MG, Dworzak MN, Ratei R, Silvestri D, Benetello A, Buldini B, Maglia O, Masera G, Conter V, Arico M, Biondi A, Gaipa G. Risk of relapse of childhood acute lymphoblastic leukemia is predicted by flow cytometric measurement of residual disease on day 15 bone marrow. *J Clin Oncol.* 2009;27:5168–5174.
- Gaipa G, Basso G, Biondi A, Campana D. Detection of minimal residual disease in pediatric acute lymphoblastic leukemia. *Cytom Part B Clin Cytom.* 2013;84:359–369.
- Campana D, Coustan-Smith E. Advances in the immunological monitoring of childhood acute lymphoblastic leukaemia. *Best Pract Res Clin Haematol.* 2002;15:1–19.
- Huh D, Gu W, Kamotani Y, Grotberg JB, Takayama S. Microfluidics for flow cytometric analysis of cells and particles. *Physiol Meas.* 2005;26.
- Hua Z, Rouse JL, Eckhardt AE, Srinivasan V, Pamula VK, Schell WA, Benton JL, Mitchell TG, Pollack MG. Multiplexed real-time polymerase chain reaction on a digital microfluidic platform. *Anal Chem.* 2010;82:2310–2316.
- Chen J, Li J, Sun Y. Microfluidic approaches for cancer cell detection, characterization, and separation. *Lab Chip.* 2012;12:1753–1767.
- Stott SL, Hsu C-H, Tsukrov DI, Yu M, Miyamoto DT, Waltman BA, Rothenberg SM, Shah AM, Smas ME, Korir GK, Floyd FP, Gilman AJ, Lord JB, Winokur D, Springer S, Irimia D, Nagrath S, Sequist LV, Lee RJ, Isselbacher KJ, Maheswaran S, Haber DA, Toner M. Isolation of circulating tumor cells using a microvortex-generating herringbone-chip. *Proc Natl Acad Sci USA.* 2010;107:18392–18397.
- Ferreira MM, Romani VC, Jeffrey SS. Circulating tumor cell technologies. *Mol Oncol.* 2016;10:374–394.
- Saliba A-E, Saias L, Psychari E, Minc N, Simon D, Bidard F-C, Mathiot C, Pierga J-Y, Fraissier V, Salamero J, Saada V, Farace F, Vielh P, Malaquin L, Viovy J-L. Microfluidic sorting

- and multimodal typing of cancer cells in self-assembled magnetic arrays. *Proc Natl Acad Sci USA*. 2010;107:14524–14529.
12. Chang C, Jalal SI, Huang W, Mahmood A, Matei DE, Savran CA. High-throughput immunomagnetic cell detection using a microaperture chip system. *IEEE Sens J*. 2014;14:3008–3013.
 13. Issadore D, Chung J, Shao H, Liong M, Ghazani AA, Castro CM, Weissleder R, Lee H. Ultrasensitive clinical enumeration of rare cells ex vivo using a micro-hall detector. *Sci Transl Med*. 2012;4.
 14. Icoz K, Iverson BD, Savran C. Noise analysis and sensitivity enhancement in immunomagnetic nanomechanical biosensors. *Appl Phys Lett*. 2008;93.
 15. Icoz K, Savran C. Nanomechanical biosensing with immunomagnetic separation. *Appl Phys Lett*. 2010;97:123701.
 16. İçöz K, Mzava O. Detection of proteins using nano magnetic particle accumulation-based signal amplification. *Appl Sci*. 2016;6:394.
 17. Mzava O, Taş Z, İçöz K. Magnetic micro/nanoparticle flocculation-based signal amplification for biosensing. *Int J Nanomed*. 2016;11:2619–2631.
 18. Jayamohan H, Gale BK, Minson B, Lambert CJ, Gordon N, Sant HJ. Highly sensitive bacteria quantification using immunomagnetic separation and electrochemical detection of guanine-labeled secondary beads. *Sensors*. 2015;15:12034–12052.
 19. Wang D, Wang Z, Chen J, Kinchla AJ, Nugen SR. Rapid detection of *Salmonella* using a redox cycling-based electrochemical method. *Food Control*. 2016;62:81–88.
 20. van Dongen JJM, van der Velden VHJ, Brüggemann M, Orfao A. Minimal residual disease diagnostics in acute lymphoblastic leukemia: need for sensitive, fast, and standardized technologies. *Blood*. 2015;125:3996–4009.
 21. Sun C, Hsieh Y-P, Ma S, Geng S, Cao Z, Li L, Lu C. Immunomagnetic separation of tumor initiating cells by screening two surface markers. *Sci Rep*. 2017;7:40632.
 22. Li J, Thielemann C, Reuning U, Johannsmann D. Monitoring of integrin-mediated adhesion of human ovarian cancer cells to model protein surfaces by quartz crystal resonators: evaluation in the impedance analysis mode. *Biosens Bioelectron*. 2005;20:1333–1340.
 23. Braunhut SJ, McIntosh D, Vorotnikova E, Zhou T, Marx KA. Detection of apoptosis and drug resistance of human breast cancer cells to taxane treatments using quartz crystal microbalance biosensor technology. *Assay Drug Dev Technol*. 2005;3:77–88.
 24. Barber N, Gez S, Belov L, Mulligan SP, Woolfson A, Christopherson RI. Profiling CD antigens on leukaemias with an antibody microarray. *FEBS Lett*. 2009;583:1785–1791.
 25. Villablanca JG, Anderson JM, Moseley M, Law CL, Elstrom RL, LeBien TW. Differentiation of normal human pre-B cells *in vitro*. *J Exp Med*. 1990;172:325–334.
 26. Icoz K, Soyul MC, Canikara Z, Unal E. Quartz-crystal microbalance measurements of CD19 antibody immobilization on gold surface and capturing B lymphoblast cells: effect of surface functionalization. *Electroanalysis*. 2018;30:834–841.
 27. Chu IM, Hsu SG, Yeh HM, Chen PM. Analysis of the immunomagnetic adhesion of the common acute lymphoblastic leukemia antigen-carrying cells. *J Ferment Bioeng*. 1996;81:367–373.
 28. Campana D, Coustan-Smith E, Manabe A, Buschle M, Raimondi SC, Behm FG, Ashmun R, Aricò M, Biondi A, Pui CH. Prolonged survival of B-lineage acute lymphoblastic leukemia cells is accompanied by overexpression of bcl-2 protein. *Blood*. 1993;81:1025–1031.
 29. Atta J, Fauth F, Keyser M, Petershofen E, Weber C, Lippok G, Hoelzer D, Martin H. Purging in BCR-ABL-positive acute lymphoblastic leukemia using immunomagnetic beads: comparison of residual leukemia and purging efficiency in bone marrow vs peripheral blood stem cells by semiquantitative polymerase chain reaction. *Bone Marrow Transplant*. 2000;25:97–104.
 30. Dakka N, Bellaoui H, Bouzid N, Khattab M, Bakri Y, Benjouad A. CD10 and CD34 expression in childhood acute lymphoblastic leukemia in Morocco: clinical relevance and outcome. *Pediatr Hematol Oncol*. 2009;26:251–266.
 31. Ichii M, Oritani K, Yokota T, Zhang Q, Garrett KP, Kanakura Y, Kincade PW. The density of CD10 corresponds to commitment and progression in the human B lymphoid lineage. *PLoS ONE*. 2010;5.
 32. Varshney M, Yang L, Su X-L, Li Y. Magnetic nanoparticle-antibody conjugates for the separation of *Escherichia coli* O157:H7 in ground beef. *J Food Prot*. 2005;68:1804–1811.
 33. Brandão D, Liébana S, Campoy S, Alegret S, Pividori MI. Immunomagnetic separation of *Salmonella* with tailored magnetic micro and nanocarriers. A comparative study. *Talanta*. 2015;143:198–204.
 34. Chen J, Park B. Effect of immunomagnetic bead size on recovery of foodborne pathogenic bacteria. *Int J Food Microbiol*. 2018;267:1–8.
 35. Matsunaga T, Suzuki T, Tanaka M, Arakaki A. Molecular analysis of magnetotactic bacteria and development of functional bacterial magnetic particles for nano-biotechnology. *Trends Biotechnol*. 2007;25:182–188.
 36. Leyendeckers H, Tasanen K, Bruckner-Tuderman L, Zillikens D, Sitaru C, Schmitz J, Hunzelmann N. Memory B cells specific for the NC16A domain of the 180 kDa bullous pemphigoid autoantigen can be detected in peripheral blood of bullous pemphigoid patients and induced *in vitro* to synthesize autoantibodies. *J Invest Dermatol*. 2003;120(3):372–378.
 37. Letzkus M, Luesink E, Starck-Schwartz S, Bigaud M, Mirza F, Hartmann N, Gerstmayer B, Janssen U, Scherer A, Schumacher MM, Verles A, Vitaliti A, Nirmala N, Johnson KJ, Staedtler F. Gene expression profiling of immunomagnetically separated cells directly from stabilized whole blood for multicenter clinical trials. *Clin Transl Med*. 2014;3:36. <https://doi.org/10.1186/s40169-014-0036-z>.
 38. Iinuma H, Okinaga K, Adachi M, Suda K, Sekine T, Sakagawa K, Baba Y, Tamura J, Kumagai H, Ida A. Detection of tumor cells in blood using CD45 magnetic cell separation followed by nested mutant allele-specific amplification of p53 and K-ras genes in patients with colorectal cancer. *Int J Cancer*. 2000;89:337–344.
 39. Bilkenroth U, Taubert H, Riemann D, Rebmann U, Heynemann H, Meye A. Detection and enrichment of disseminated renal carcinoma cells from peripheral blood by immunomagnetic cell separation. *Int J Cancer*. 2001;92(4):577–582. <https://doi.org/10.1002/ijc.1217>.
 40. Recktenwald D, Radbruch A. *Cell Separation Methods and Applications*. New York, NY; 1997.
 41. Grützkau A, Radbruch A. Small but mighty: how the MACS1-technology based on nanosized superparamagnetic particles has helped to analyze the immune system within the last 20 years. *Cytom Part A*. 2010;77(7):643–647. <https://doi.org/10.1002/cyto.a.20918>.
 42. Goddard RV, Prentice AG, Copplestone JA, Kaminski ER. Generation *in vitro* of B-cell chronic lymphocytic leukaemia-proliferative and specific HLA class-II-restricted cytotoxic T-cell responses using autologous dendritic cells pulsed with tumour cell lysate. *Clin Exp Immunol*. 2001;126(1):16–18.
 43. Kuhara M, Takeyama H, Tanaka T, Matsunaga T. Magnetic cell separation using antibody binding with protein a expressed on bacterial magnetic particles. *Anal Chem*. 2004;76(21):6207–6213. <https://doi.org/10.1021/ac0493727>.

Manuscript received Jun. 8, 2018, revision received Sep. 7, 2018, accepted Oct. 16, 2018.